Fused–Costal2 protein complex regulates Hedgehog-induced Smo phosphorylation and cell-surface accumulation

Yajuan Liu,[1,4] Xuesong Cao,[1,4] Jin Jiang,[2] and Jianhang Jia[1,3,5]

[1]Sealy Center for Cancer Cell Biology, University of Texas Medical Branch, Galveston, Texas 77555, USA; [2]Center for Developmental Biology and Department of Pharmacology, University of Texas Southwestern Medical Center, Dallas, Texas 75390, USA; [3]Department of Biochemistry and Molecular Biology, University of Texas Medical Branch, Galveston, Texas 77555, USA

The seven-transmembrane protein Smoothened (Smo) acts as a signal transducer in the Hedgehog (Hh) pathway that mediates many key developmental processes. In *Drosophila*, Hh-induced phosphorylation promotes Smo cell-surface accumulation and signaling activity; however, the mechanisms controlling Smo phosphorylation and cell-surface accumulation are still unknown. The intracellular signaling complex containing Fused (Fu) and Costal2 (Cos2) is thought to transduce the Hh signal downstream from Smo. Here, we identify a novel feedback mechanism that regulates Smo through the Fu–Cos2 complex. We found that Hh-induced Smo accumulation is inhibited in *fu* mutant clones or by expressing a dominant-negative form of Fu, and such inhibition is alleviated by removal of Cos2. Conversely, overexpressing Cos2 blocks Smo accumulation, which is reversed by coexpressing Fu. Cos2 blocks Smo accumulation through its C-terminal Smo-interacting domain, and Fu antagonizes Cos2 by phosphorylating Cos2 at Ser572. Furthermore, we found that Ser572 phosphorylation attenuates the Cos2–Smo interaction and promotes Cos2 instability. Finally, we provided evidence that Fu and Cos2 control Smo cell-surface accumulation by regulating Smo phosphorylation. Our data suggest that Cos2–Smo interaction blocks Hh-induced Smo phosphorylation, and that Fu promotes Smo phosphorylation by antagonizing Cos2.

[*Keywords*: Smo; Fu; Cos2; Hh; phosphorylation; signal transduction]

Supplemental material is available at http://www.genesdev.org.

Received April 3, 2007; revised version accepted June 18, 2007.

The Hedgehog (Hh) pathway is responsible for a variety of developmental processes, including cell proliferation, embryonic patterning, and organ development (Ingham and McMahon 2001; Lum and Beachy 2004; Jia and Jiang 2006). Dysregulation of Hh signaling is associated with a wide variety of human disorders, including cancer (Taipale and Beachy 2001; Pasca di Magliano and Hebrok 2003). In the *Drosophila* wing disc, Hh is secreted by posterior (P) compartment cells (P-cells), and induces the anterior (A) compartment cells (A-cells) adjacent to the A/P boundary to express *decapentaplegic* (*dpp*), which encodes a member of the TGFβ/BMP family of secreted proteins (Ingham and McMahon 2001). The Dpp protein then diffuses into both the A- and P-compartments and functions as a long-range morphogen to control the growth and patterning of cells in the entire wing (Ingham and McMahon 2001). Hh also specifies cell patterning near the A/P boundary by functioning as a local morphogen. Low levels of Hh are able to induce the expression of *dpp*, whereas higher levels of Hh are required to activate *ptc*. The induction of *en* requires peak levels of Hh signaling activities (Strigini and Cohen 1997). Thus, the levels of Hh signaling activity can be monitored by the expression of different responsive genes.

The Hh signal is transduced through a reception system that includes the 12-span transmembrane protein Patched (Ptc) and seven-span transmembrane Smoothened (Smo). In the absence of Hh, Ptc inhibits Smo. Binding of Hh to Ptc alleviates such inhibition, allowing Smo to regulate the Cubitus interruptus (Ci)/Gli family of Zn-finger transcription factors (Ingham and McMahon 2001).

How Smo signaling activity is regulated remains poorly understood. In *Drosophila*, Hh induces Smo phosphorylation and cell-surface accumulation (Denef et al. 2000). We and others have identified PKA and CKI as two of the kinases that phosphorylate Smo and increase its cell-surface localization and signaling activity (Jia et al. 2004; Zhang et al. 2004; Apionishev et al. 2005). Block-

[4]These authors contributed equally to this work.
[5]Corresponding author.
E-MAIL jijia@UTMB.edu; FAX (409) 747-1938.
Article is online at http://www.genesdev.org/cgi/doi/10.1101/gad.1557407.

ing PKA or CKI activity prevents Hh-induced Smo accumulation on the plasma membrane and attenuates its pathway activity, whereas increasing PKA activity promotes Smo accumulation and pathway activation (Jia et al. 2004). It appears that phosphorylation is sufficient to induce Smo cell-surface accumulation and activation, as phosphorylation-mimicking Smo variants show constitutive signaling activity and cell-surface accumulation (Jia et al. 2004; Zhang et al. 2004). Despite the identification of Smo kinases, how Smo phosphorylation is regulated still remains a mystery.

The Ser/Thr kinase Fused (Fu) and the kinesin-related protein Costal2 (Cos2) exist in a large protein complex with the full-length Ci (Ci155) (Robbins et al. 1997; Sisson et al. 1997). Cos2 mainly acts as a negative regulator in the Hh signaling pathway (Sisson et al. 1997; Wang and Holmgren 2000; Wang et al. 2000; Ho et al. 2005) and inhibits the transcriptional activator activity of Ci155 by inhibiting its nuclear translocation (Chen et al. 1999; Stegman et al. 2000; Wang et al. 2000; Monnier et al. 2002). Cos2 also acts as a scaffold protein to bring PKA, CKI, and GSK3 kinases to Ci155 (Zhang et al. 2005), promoting sequential phosphorylation of Ci155 by these kinases (Price 2006), leading to proteasome-mediated Ci155 processing to generate its repressor form, Ci75 (Chen et al. 1999; Wang and Holmgren 1999; Tian et al. 2005; Wang and Li 2006). Ci75 binds DNA and represses the transcription of Hh target genes such as *dpp* (Aza-Blanc et al. 1997; Methot and Basler 1999).

Mutations in *fu* affect high-threshold Hh responses (Preat 1992; Alves et al. 1998). It has also been shown that Fu converts Ci into a hyperactive and labile form by antagonizing Su(fu) (Ohlmeyer and Kalderon 1998). The effects of Fu and Cos2 appear to be more complicated than simply acting as a pathway activator and repressor, respectively. Fu is required for Ci processing in certain genetic backgrounds (Lefers et al. 2001). On the other hand, Cos2 has a positive role in Hh-responding cells, and this correlates to its ability to form a complex with the C-terminal intracellular tail of Smo (Wang et al. 2000; Jia et al. 2003; Lum et al. 2003; Ogden et al. 2003). In addition, Fu is diminished in cells lacking Cos2 (Lum et al. 2003; Ruel et al. 2003), which might explain, at least in part, why Hh signaling activity is attenuated in *cos2* mutant cells adjacent to the A/P boundary (Ho et al. 2005). Another unexpected observation is that overexpression of Cos2 blocks Smo accumulation in P-compartment cells of wing discs (Ruel et al. 2003), implying that the Fu–Cos2 complex may play additional roles in regulating Hh signal transduction.

The mechanisms by which Fu and Cos2 are regulated by Hh also remain elusive. Both are phosphorylated in response to Hh, but the biological function of these phosphorylation events is largely unknown. Although the physiological substrate(s) for the Fu kinase is still not known, it has been shown that Su(fu) is phosphorylated in response to Hh, and this phosphorylation depends on Fu (Lum et al. 2003). However, it is not clear whether Su(fu) is a direct substrate for Fu. Another candidate for a physiological Fu substrate is Cos2. It has been shown that Fu can phosphorylate Cos2 when they are coexpressed in insect cells using the baculovirus system, and the Ser572 of Cos2 is the major site of Fu-mediated phosphorylation (Nybakken et al. 2002). Additional evidence suggests that Cos2 Ser572 phosphorylation is stimulated by Hh in S2 cells (Nybakken et al. 2002); however, the biological function of Cos2 phosphorylation by Fu remains to be determined.

In this study, we further investigated the function of Fu and Cos2 in the Hh pathway and identified a novel feedback loop in which Fu promotes Smo phosphorylation and cell-surface accumulation by antagonizing Cos2. We found that Cos2 inhibits Smo phosphorylation and cell-surface accumulation through its C-terminal Smo interaction domain, and that Fu alleviates Cos2 inhibition of Smo by phosphorylating Cos2 at Ser572.

Results

Fu^{G13V} is a dominant inhibitor of endogenous Fu

To investigate the mechanism by which the kinase Fu is involved in Hh signaling, we generated an HA-tagged Fu mutant that changes Gly13 into Val (Fu^{G13V}). This mutation occurs naturally and has been characterized as a strong allele of Class I mutations (Therond et al. 1996). Consistent with this, we found that Fu^{G13V} did not rescue the fu^A mutant phenotype when expressed under the control of a weak Gal4 driver, *armadillo*-Gal4, whereas expressing HA-tagged wild-type Fu (HA-Fu^{WT}) rescued fu^A (data not shown). To determine if Fu^{G13V} has a dominant-negative effect over the endogenous Fu, we expressed Fu^{G13V} using a strong, wing-specific driver, *MS1096* Gal4. We found that overexpression of Fu^{G13V} induced a "fused" wing phenotype (Fig. 1C) similar to that caused by the fu^A mutation (Fig. 1B). We also generated marked clones expressing Fu^{G13V} in wing discs using *act* > *CD2* > Gal4 driver and found that Fu^{G13V} blocked *ptc-lacZ* expression (Fig. 1D,D′), a phenotype similar to that caused by strong *fu* mutations (Alves et al. 1998; Methot and Basler 2000). As Fu forms a tight complex with Cos2, the nonfunctional Fu^{G13V} may compete with endogenous Fu for Cos2, leading to a *fu* mutant phenotype. If this is the case, coexpression of Fu^{WT} with Fu^{G13V} may attenuate the dominant-negative effect of Fu^{G13V} and restore Hh signaling. We thus used the wing-specific *ap*-Gal4 driver (Jia et al. 2004), which expresses Gal4 in dorsal compartment cells, to overexpress Fu^{WT} together with Fu^{G13V}. Expressing HA-Fu^{G13V} along with *ap*-Gal4 inhibited the expression of endogenous *en* in anterior–dorsal cells near the A/P boundary (Fig. 1F–F‴). Coexpressing Myc-Fu^{WT} with HA-Fu^{G13V} restored *en* expression (Fig. 1G–G″), and rescued the Fu^{G13V} wing phenotype (data not shown), suggesting that HA-Fu^{G13V} can interfere with the endogenous Fu in transducing high-level Hh signaling activity.

Fu is essential for Hh-induced Smo accumulation

Smo, Fu, and Cos2 form a large protein complex involved in Hh signal transduction (Jia et al. 2003; Lum et al.

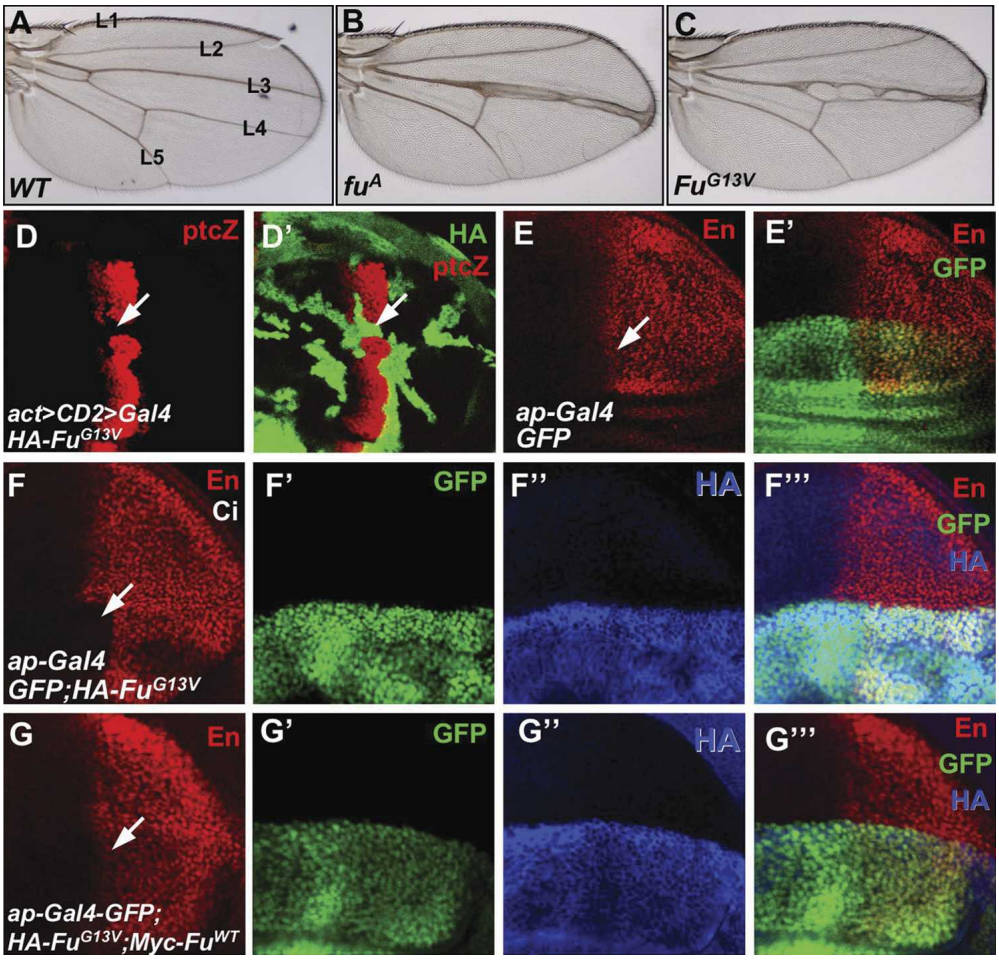

Figure 1. Fu^{G13V} has a dominant-negative effect in Hh pathway. (*A–C*) Adult wings from wild-type (*A*), fu^{A} mutant (*B*), or flies expressing HA-Fu^{G13V} by *MS1096* Gal4 (*C*). Note the fusion between L3 and L4 in fu^{A}- and Fu^{G13V}-expressing wings. (*D,D′*) A wing disc expressing HA-Fu^{G13V} with *act* > *CD2* > Gal4 was immunostained for HA (green) and *ptc-lacZ* (red). Fu^{G13V} blocked *ptc-lacZ* expression (arrows). (*E,E′*) A wing disc expressing GFP (green) with *ap*-Gal4 was immunostained to show the expression of En (red). (*F–F‴*) A wing disc expressing GFP (green) and HA-Fu^{G13V} with *ap*-Gal4 was immunostained to show the expression of En (red) and HA (blue). Expressing HA-Fu^{G13V} inhibited the expression of *en* in anterior dorsal cells near the A/P boundary (arrow in *F*). (*G–G‴*) A wing disc coexpressing Myc-Fu^{WT} with HA-Fu^{G13V} restored anterior dorsal En expression (arrow in *G*) that was inhibited by Fu^{G13V}. All wing discs shown in this study were oriented with anterior to the left and ventral on the top.

2003; Ogden et al. 2003; Ruel et al. 2003). To determine if Fu could regulate Smo, we examined Smo distribution in wing discs expressing HA-Fu^{G13V} with *ap*-Gal4. Surprisingly, overexpressing the dominant-negative form of Fu blocked Hh-induced elevation of Smo in P-cells, as well as in A-cells adjacent to the A/P boundary (Fig. 2B), suggesting that Fu activity is required for Hh-induced Smo accumulation.

To investigate whether the blockade of Smo accumulation by Fu^{G13V} is due to preventing Smo cell-surface localization, we turned to a cell-based assay we established earlier for studying Smo cell-surface accumulation (Jia et al. 2004). S2 cells were transfected with CFP-Smo with or without Fu^{G13V}, or with Fu^{WT}, and then treated with Hh-conditioned or control medium. To visualize cell-surface-localized Smo, we stained cells with an anti-SmoN antibody before cell permeabilization (Jia et al. 2004). Consistent with our previous findings (Jia et al. 2004), Smo accumulated on the cell surface upon Hh stimulation (Fig. 2C,D). The Hh-induced CFP-Smo cell-surface accumulation was blocked by expressing Fu^{G13V} (Fig. 2H), but not by expressing Fu^{WT} (data not shown), suggesting that the attenuation of Smo levels by Fu^{G13V} is due to blocking Smo cell-surface accumulation.

Smo cell-surface accumulation is promoted by Hh-induced phosphorylation at three clusters of PKA and CKI sites (Jia et al. 2004; Zhang et al. 2004; Apionishev et al. 2005). We have previously shown that Smo^{SD123}, in which the three clusters of PKA and CKI phosphorylation sites are replaced by Asp to mimic phosphorylation, has constitutive cell-surface expression and signaling activity (Jia et al. 2004). To determine if Fu^{G13V} could block the cell-surface localization of Smo^{SD123}, S2 cells were transfected with Smo^{SD123} and Fu^{G13V}, then treated with Hh-conditioned or control medium. Strikingly, the constitutive cell-surface accumulation of Smo^{SD123} was not

affected by Fu^{G13V} (Fig. 2J), even in the absence of Hh (Fig. 2I). Thus, the phosphorylation-mimicking form of Smo escaped regulation by Fu, suggesting that Fu^{G13V} may block Smo cell-surface accumulation by preventing Smo phosphorylation (see below).

The blockade of Smo accumulation by Fu^{G13V} is mediated by Cos2

Several lines of evidence suggest that Cos2 may be involved in the regulation of Smo by Fu. First, we and others have shown a physical interaction between Smo and the Fu/Cos2 complex (Jia et al. 2003; Lum et al. 2003; Ogden et al. 2003; Ruel et al. 2003), likely through a direct association with Cos2 (Lum et al. 2003; Ogden et al. 2003). Second, Cos2 can be phosphorylated by Fu (Nybakken et al. 2002). Third, Cos2 is accumulated in P-cells in which Fu activity is compromised by Fu^{G13V} overexpression (see below). Finally, overexpression of Cos2 blocked Smo accumulation in P-cells (Fig. 4A, below; Ruel et al. 2003), phenocopying loss of Fu activity. To test our hypothesis, Fu^{G13V} was expressed under the control of the wing-specific *MS1096* Gal4 driver in *cos2* mutant wing discs. As shown in Figure 3, Fu^{G13V} blocked Smo accumulation in the *cos2* heterozygous disc ($cos2^{-/+}$) (Fig. 3A–A‴), but not in the *cos2* homozygous disc ($cos2^{-/-}$) (Fig. 3B–B‴), suggesting that Cos2 is required for Fu^{G13V} to inhibit Smo.

To determine whether the effect of Fu^{G13V} on Smo cell-surface accumulation in S2 cells relies on Cos2, we used double-stranded RNA (dsRNA) to knock down endogenous Cos2. We found that Hh induced Smo cell-surface accumulation in the presence of Fu^{G13V} when Cos2 was knocked down by RNA interference (RNAi) (Fig. 3E), indicating that the effect of Fu^{G13V} on Smo accumulation was dependent on Cos2.

To confirm the physiological regulation of Smo by Fu and Cos2, we turned to *fu* and *cos2* loss-of-function mutants. We examined Smo distribution in wing discs carrying mutant clones homozygous for a strong *fu* allele, fu^{mH63} (a Class I allele), and found that Smo accumulation was blocked in *fu* mutant cells situated in A-cells near the A/P boundary (Fig. 3C), suggesting that Fu activity is essential for Hh-induced Smo accumulation. Significantly, the down-regulation of Smo by the *fu* mutation was alleviated by the loss of *cos2*, as Hh-induced

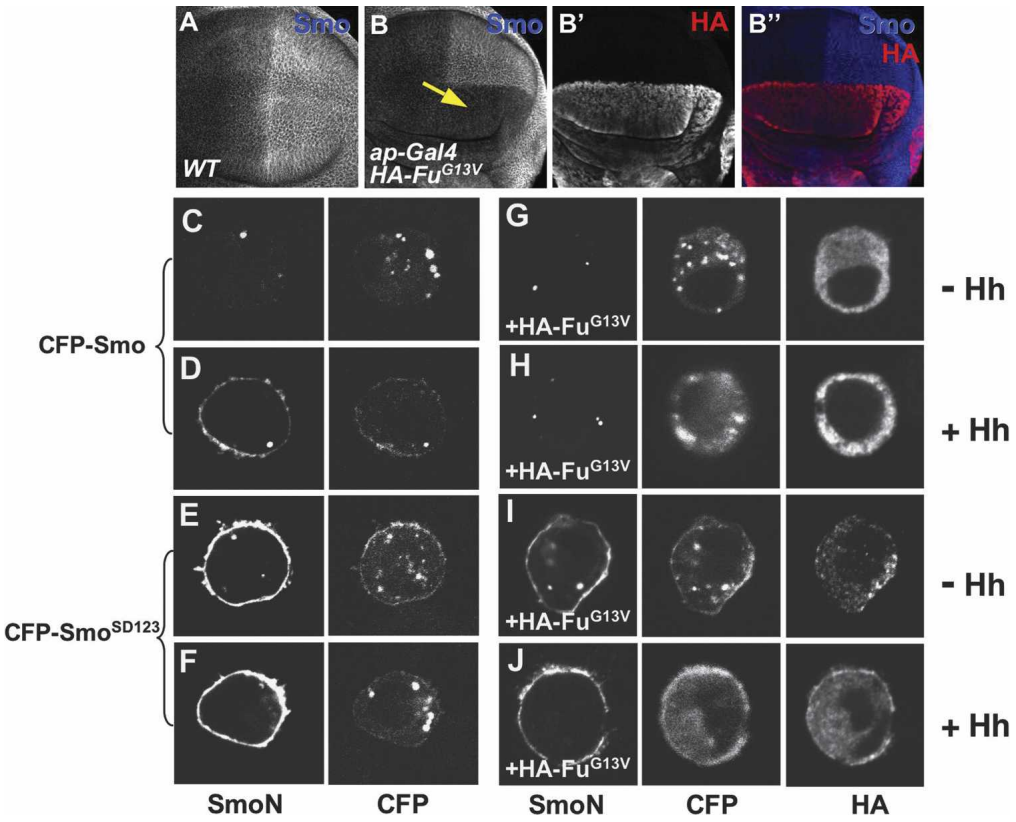

Figure 2. Fu is required for Hh-induced Smo accumulation. (*A*) A wild-type wing disc was immunostained to show Hh-induced Smo accumulation in P-cells. (*B–B″*) Expression of Fu^{G13V} (red) with *ap*-Gal4 blocked Smo accumulation in the dorsal compartment cells (arrow in *B*). (*C–F*) S2 cells were transfected with CFP-tagged Smo (*C,D*) or Smo^{SD123} (*E,F*) and treated with Hh-conditioned medium (*D,F*) or control medium (*C,E*). (*G–J*) S2 cells were cotransfected with HA-Fu^{G13V} plus either CFP-Smo (*G,H*) or CFP-Smo^{SD123} (*I,J*), followed by treatment with Hh-conditioned medium (*H,J*) or control medium (*G,I*). Fu^{G13V} blocked Hh-induced CFP-Smo cell-surface accumulation (*H*) but did not block CFP-Smo^{SD123} accumulation (*I,J*). SmoN antibody staining indicates the cell-surface-localized Smo, and CFP signal indicates the total amount of expressed Smo.

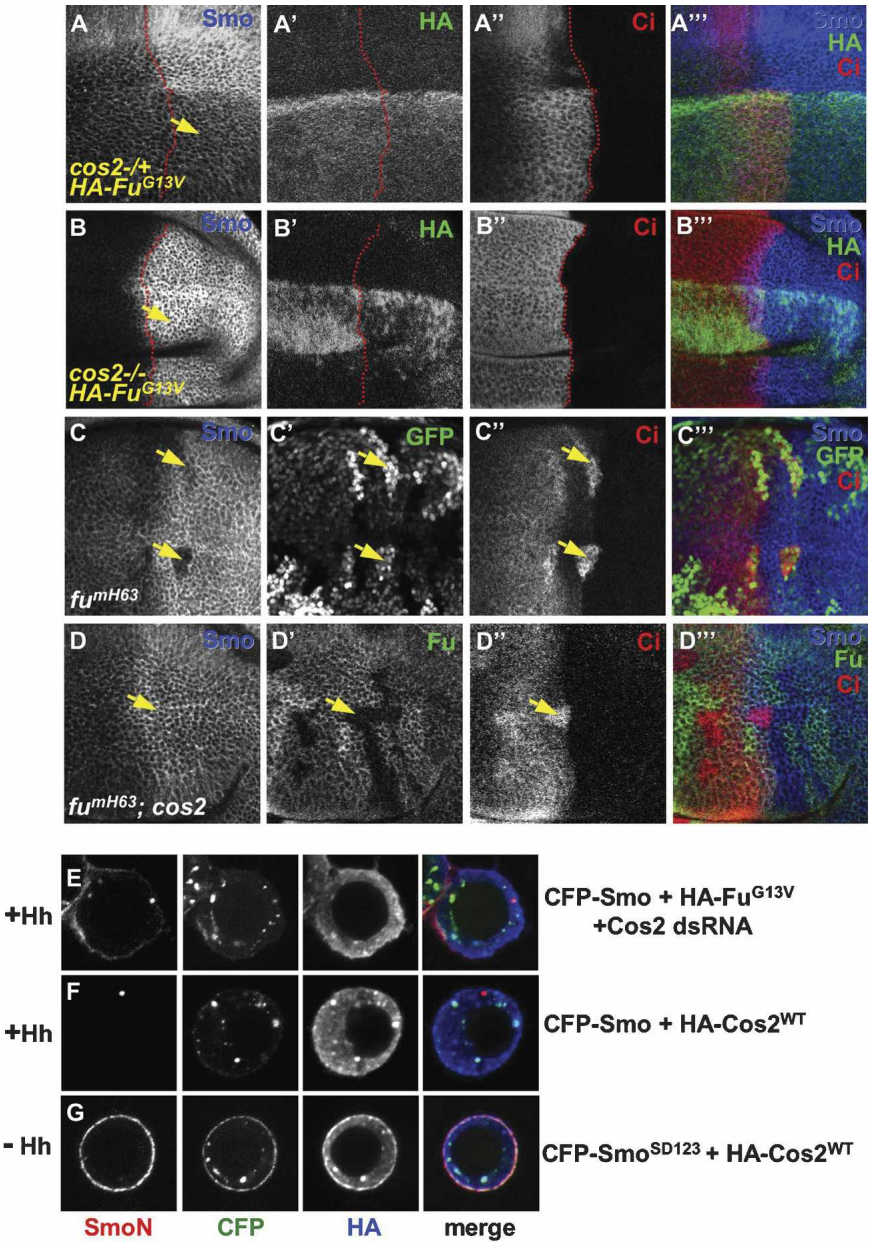

Figure 3. Fu regulates Smo through Cos2. (*A–B‴*) *cos2* mutant discs were immunostained with anti-SmoN (blue), anti-HA (green), and anti-Ci (red) antibodies to show the effect of Fu^{G13V} on Smo accumulation. A *cos2* heterozygous (+/–) wing disc expressing HA-Fu^{G13V} under *MS1096* Gal4 showed attenuated Smo accumulation indicated by Smo staining in P-cells (arrow in *A*), whereas Smo accumulation was unaffected in a *cos2* homozygous (–/–) disc expressing HA-Fu^{G13V} (arrow in *B*). The elevated Ci staining in *A″* and *B″* was due to the expression of the Fu^{G13V} and *cos2* mutations, respectively. Of note, *MS1096* expresses higher levels of Gal4 in dorsal compartment cells than in ventral compartment cells. The A/P boundary was outlined by a red line according to the Ci expression domain. (*C–C‴*) Wing disc containing *fu* mutant clones was immunostained to show the decrease in Smo levels (arrows in *C*). *fu* mutant clones were recognized by two copies of GFP expression (arrow in *C′*). (*D–D‴*) Wing disc containing *fu cos2* double-mutant clones was immunostained to show the restored Smo levels (arrow in *D*). *fu* and *cos2* mutant clones were recognized by staining with anti-Fu antibody (arrow in *D′*). (*E*) S2 cells were cotransfected with CFP-Smo and HA-Fu^{G13V}, plus Cos2 dsRNA followed by treatment with Hh-conditioned medium. Hh-induced Smo cell-surface accumulation was recovered by knocking down endogenous Cos2. (*F*,*G*) S2 cells were cotransfected with HA-$Cos2^{WT}$ plus either CFP-Smo^{SD123} or CFP-Smo, followed by Hh-treatment. Cos2 blocked Hh-induced CFP-Smo cell-surface accumulation (*F*) but did not block CFP-Smo^{SD123} accumulation (*G*).

Smo accumulation was restored in *fu cos2* double-mutant clones (Fig. 3D). We also found that *fu cos2* double clones show normal Smo levels in both A- and P-compartments (data not shown). Taken together, these observations suggest that Cos2 is responsible for blocking Hh-induced Smo accumulation when Fu activity is compromised.

The C-terminal region of Cos2 mediates its inhibition of Smo accumulation

The above data suggest that Cos2 may prevent Smo cell-surface accumulation, whereas Fu activity is normally required to overcome this blockade. Consistent with this, overexpression of Cos2 down-regulates Smo in wing discs (Fig. 4A; Ruel et al. 2003). To further test this hypothesis and determine whether down-regulation of Smo cell-surface expression by Cos2 depended on the Smo phosphorylation status, we cotransfected S2 cells with CFP-Smo or CFP-Smo^{SD123} together with Cos2, followed by treatment with Hh-conditioned medium. As shown in Figure 3F, Hh-induced CFP-Smo cell-surface accumulation was blocked by Cos2 coexpression. In contrast, coexpression of Cos2 had no effect on CFP-Smo^{SD123} cell-surface accumulation (Fig. 3G), as was the case with Fu^{G13V} coexpression, implying that Cos2 prevented Smo accumulation at a step prior to Smo phosphorylation.

To define the Cos2 domain(s) responsible for inhibiting Smo, we tested a set of Cos2 deletion mutants (Fig.

4G) in wing discs to assess their ability to down-regulate Smo. We found that a Cos2 mutant with its C-tail deleted (Cos2ΔC1) no longer blocked Smo accumulation (Fig. 4D). In contrast, deletion of the microtubule-binding domain alone (Cos2ΔN1) or together with the neck region (Cos2ΔN2) did not affect the ability of the resulting Cos2 mutants to block Smo accumulation (Fig. 4B,C, respectively). In addition, we found that the Cos2 C-tail (Cos2CT) alone was sufficient to block Smo (Fig. 4F). Consistent with a recent finding that expression of a Cos2 C-terminal domain disrupts Hh signaling (Ogden et al. 2006), we found that the overexpression of Cos2CT in imaginal discs diminished *ptc* expression in A-cells adjacent to the A/P boundary (data not shown). We further examined the Cos2 deletion mutants in S2 cells and found their ability to prevent Smo cell-surface accumulation in S2 cells (Supplementary Fig. S1) correlated with their ability to down-regulate Smo in wing discs.

Cos2 blocks Smo phosphorylation

Neither Cos2 nor Fu^{G13V} blocked Smo^{SD123} cell-surface accumulation, suggesting that the Fu–Cos2 complex may regulate Smo accumulation by regulating its phos-

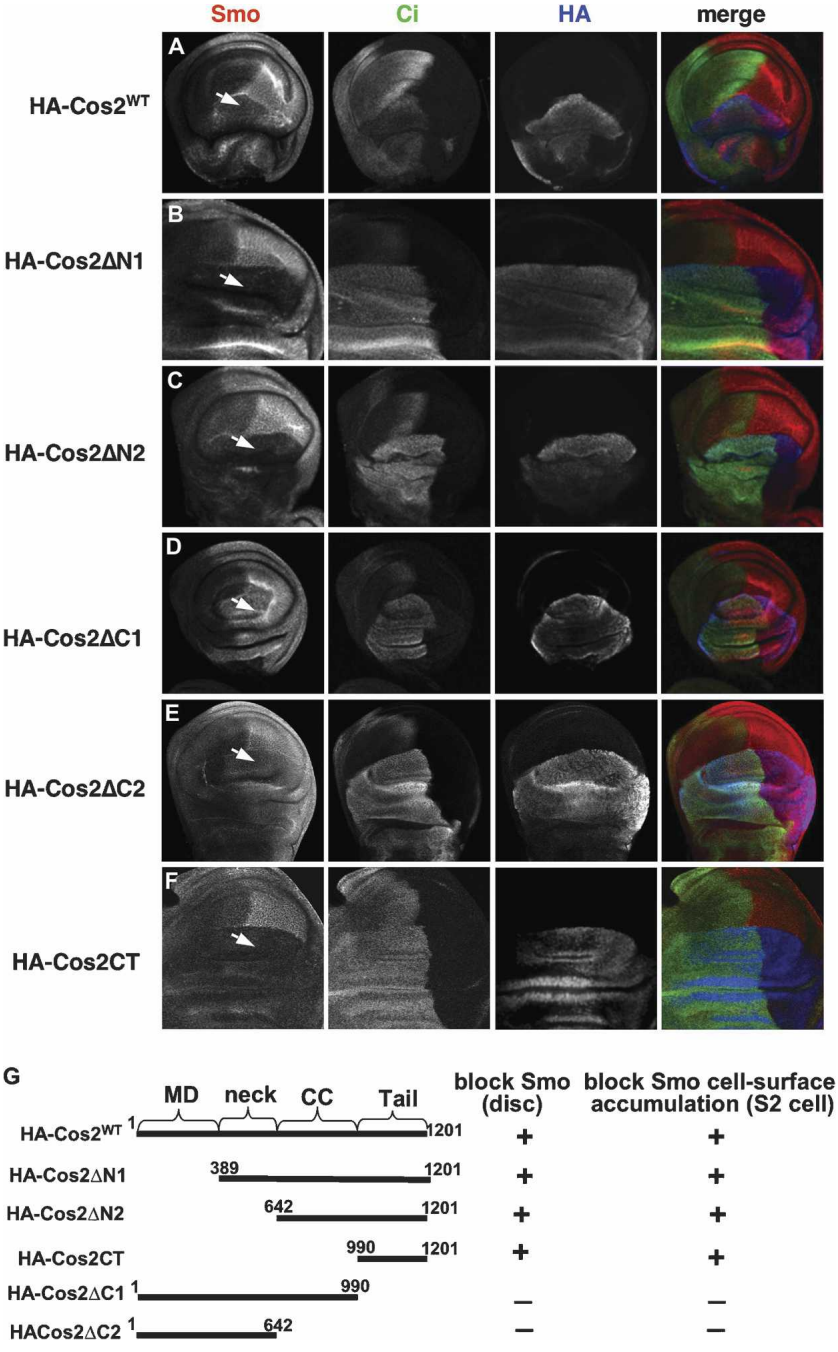

Figure 4. The ability of Cos2 deletion mutants to block Smo accumulation. (*A–F*) Wing discs expressing HA-tagged Cos2 variants by *ap*-Gal4 were immunostained with anti-HA (blue), anti-Ci (green), and anti-SmoN (red) antibodies to show the ability of Cos2 deletion mutants to inhibit Smo. Arrows indicate Smo levels in dorsal P-cells. (*G*) Schematic drawing of Cos2 constructs with their ability to down-regulate Smo accumulation indicated.

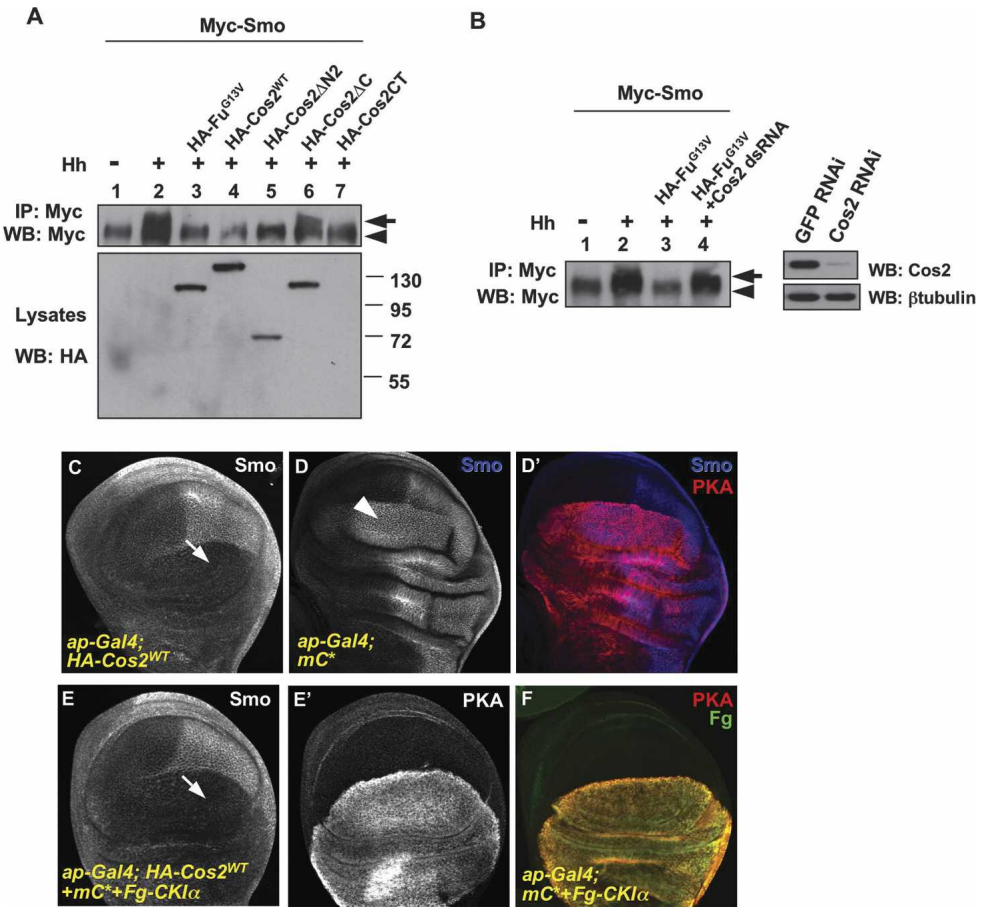

Figure 5. Cos2 blocks Smo phosphorylation. (*A*) S2 cells were transfected with the indicated constructs and treated with Hh-conditioned or control medium. (*Top* panel) Cell extracts were immunoprecipitated with anti-Myc antibody followed by Western blot with anti-Myc antibody to detect the phosphorylation status of Smo. The arrow indicates hyperphosphorylated forms of Smo and the arrowhead indicates hypophosphorylated and unphosphorylated forms. (*Bottom* panel) The expression of individual Cos2 constructs was detected by direct Western blot with anti-HA antibody. Of note, Cos2CT ran out of the gel due to its small molecular weight (27 kDa). (WB) Western blot. (*B*, lane *4*) S2 cells were cotransfected with Myc-Smo, HA-Fu^{G13V}, and Cos2 dsRNA followed by treatment with Hh-conditioned medium to detect the effect of Cos2 RNAi (cf. lane *3* without RNAi). (Lanes *1*,*2*) S2 cells transfected with Myc-Smo followed by treatment with Hh-conditioned or control medium served as control. The inhibitory efficiency of Cos2 RNAi is shown in the *right* panel. (*C*) A wing disc overexpressing HA-Cos2^{WT} driven by *ap*-Gal4 was immunostained with anti-SmoN antibody to show the blockade of Smo accumulation in dorsal P-cells (arrow). (*D*,*D*′) A wing disc overexpressing a strong line of mC* was stained with anti-SmoN (blue) and anti-PKA (red) to show Smo expansion in A-cells near the A/P boundary (arrowhead). (*E*,*E*′) A wing disc coexpressing HA-Cos2^{WT}, mC*, and Fg-CKIα was immunostained with anti-SmoN (*E*) and anti-PKA (*E*′) antibodies. (*F*) A control disc indicates the coexpression of PKA (red) and Fg-CKIα (green) for the experiment in *E* and *E*′.

phorylation. To test this, we transfected S2 cells with Myc-tagged Smo plus HA-tagged full-length or truncated forms of Cos2 and treated the transfected cells with Hh-conditioned or control medium. Myc-Smo was immunoprecipitated from cell extracts with an anti-Myc antibody, followed by Western blot with the anti-Myc antibody. Consistent with previous findings (Denef et al. 2000; Jia et al. 2004; Zhang et al. 2004; Apionishev et al. 2005), Hh induced an electrophoretic mobility shift of Myc-Smo, indicative of Smo phosphorylation (Fig. 5A, lane 2). The Hh-induced Smo mobility shift was diminished by the coexpression of HA-Cos2^{WT}, Cos2ΔN2, or Cos2CT (Fig. 5A, lanes 4,5,7), which also blocked Smo accumulation (Fig. 4). In contrast, Smo phosphorylation was not blocked by Cos2ΔC (Fig. 5, lane 6). We also found that Fu^{G13V} blocked Smo phosphorylation (Fig. 5, lane 3). Consistent with our finding that Cos2 knockdown by RNAi restored Smo cell-surface accumulation that was inhibited by Fu^{G13V} (Fig. 3E), we found that Cos2 RNAi elevated Smo phosphorylation in the presence of Fu^{G13V} (Fig. 5B, lane 4, left panel). The Cos2 RNAi efficiency is shown in Figure 5B (right panel). Taken together, these data suggest that Fu–Cos2 controls Smo accumulation by regulating Smo phosphorylation.

It has been shown that Hh-induced Smo phosphorylation is mediated by PKA and CKI (Jia et al. 2004; Zhang et al. 2004; Apionishev et al. 2005). As the Cos2 C-terminal region also binds the PKA catalytic subunit and CKI in addition to Smo (Zhang et al. 2005), a trivial ex-

planation is that an excess amount of Cos2 blocks Smo phosphorylation by titrating out PKA and CKI. If so, one would expect that supplying excess amounts of PKA and CKI should reverse the blockade of Smo phosphorylation by Cos2. To test this, we coexpressed PKA and CKI with Cos2. Overexpressing Cos2 depleted Smo in dorsal P-cells (Fig. 5C) that was not rescued by the coexpression of a strong line of a constitutively active form of PKA catalytic subunit (mC*) and Flag-tagged CKIα (Fg-CKIα) (Fig. 5E), even though the overexpression of mC* alone resulted in a dramatic anterior expansion of the domain that accumulated high levels of Smo (Fig. 5D). These results suggest that Cos2 does not simply block Smo phosphorylation by titrating out the kinases.

Hh-induced Smo accumulation requires Cos2 phosphorylation by Fu

The requirement of Cos2 in blocking Smo accumulation when Fu activity is compromised suggests that Fu promotes Smo phosphorylation and accumulation by antagonizing Cos2. A previous study suggested that Cos2 acts downstream from Fu, as the *fu* mutant phenotype was partially suppressed by a *cos2* mutation (Preat et al. 1993). It has been also shown that Fu binds to the neck region of Cos2 (Monnier et al. 2002; Wang and Jiang 2004). Fu^{WT} but not Fu^{G13V} phosphorylates Cos2 Ser572 in the neck domain, and Ser 572 phosphorylation appears to be a critical phosphorylation event induced by Hh in S2 cells (Nybakken et al. 2002). To determine if Fu regulated Cos2 activity by phosphorylating Ser572, we generated Fu phosphorylation-mimicking ($Cos2^{S572D}$) and phosphorylation-deficient ($Cos2^{S572A}$) forms of Cos2. We analyzed Cos2 phosphorylation by using Fu^{WT}, Fu^{G13V}, or Fu RNAi. We confirmed that Ser572 was critical for Hh-induced Cos2 phosphorylation, as $Cos2^{S572A}$ exhibited a faster-migrating, unphosphorylated form whereas Cos2 exhibited a mobility shift in the presence of Hh (Fig. 6A, cf. lanes 2 and 6). Furthermore, we found that Fu was responsible for Cos2 phosphorylation, as perturbation of endogenous Fu kinase activity by either coexpression of Fu^{G13V} or Fu RNAi abolished Cos2 phosphorylation (Fig. 6A, lanes 7–10). Confirmation of effective knockdown of Fu by RNAi is shown in Figure 6A (right panel).

We next examined the in vivo effect of Ser572 phosphorylation on Smo accumulation by overexpressing HA-$Cos2^{WT}$, $Cos2^{S572A}$, or HA-$Cos2^{S572D}$ in wing discs via *ap*-Gal4. We found that $Cos2^{S572A}$ behaved like $Cos2^{WT}$, as dorsal P-cells expressing $Cos2^{S572A}$ abolished Smo accumulation (Fig. 6C). In contrast, expressing $Cos2^{S572D}$ did not prevent Smo accumulation (Fig. 6D). We further found that the effects of the exogenously expressed $Cos2^{WT}$ and $Cos2^{S572A}$ on Smo accumulation were independent of endogenous Cos2 protein (Supplementary Fig. S3). Furthermore, we found that $Cos2^{S572D}$ had a dominant-negative effect over endogenous Cos2 activity because anterior-situated clones expressing HA-$Cos2^{S572D}$ induced ectopic Ptc expression (Supplementary Fig. S2D,D′), similar to the effect of $Cos2^{S182N}$ (Ho et al. 2005). We also found that $Cos2^{S572D}$ neutralized the Fu^{G13V} effect of inhibiting Smo accumulation (Fig. 6E–E″), likely by forming an inactive heterodimer with endogenous Cos2 and/or titrating out Fu^{G13V}.

Consistent with its failure to block Smo accumulation, $Cos2^{S572D}$ also failed to block Hh-induced Smo phosphorylation in S2 cells (Fig. 6F, lane 5, top panel). In contrast, $Cos2^{S572A}$ behaved like $Cos2^{WT}$ in preventing Smo phosphorylation (Fig. 6F, lane 4, top panel). We further found that $Cos2\Delta C1^{S572A}$ and $Cos2\Delta C1^{S572D}$ behaved like Cos2ΔC1 and did not block Smo phosphorylation (data not shown) and cell-surface accumulation (Supplementary Fig. S1), further strengthening the view that the Cos2CT is essential for Cos2 to block Smo phosphorylation and accumulation.

We found that the blockade of Hh-induced Smo cell-surface accumulation by Cos2 in S2 cells was alleviated by coexpressing Fu^{WT} (Fig. 6G), but not the kinase-dead Fu mutant Fu^{G13V} (Fig. 6H), suggesting that Fu antagonizes Cos2 to promote Smo cell-surface accumulation through its kinase activity. If phosphorylation of Ser572 by Fu is essential for preventing Cos2 from inhibiting Smo, we would expect that $Cos2^{S572A}$ should be resistant to Fu^{WT} coexpression. Indeed, $Cos2^{S572A}$ dominantly blocked Smo accumulation even in the presence of Fu^{WT} coexpression (Fig. 6I). Consistently, inhibition of Hh-induced Smo phosphorylation by $Cos2^{WT}$ was eliminated by Fu^{WT} (Supplementary Fig. S5C). Taken together, these observations suggest that the negative effect of Cos2 on Hh-induced Smo phosphorylation and cell-surface expression is abolished by Fu phosphorylation of Cos2 at Ser572.

Phosphorylation of Cos2 at Ser 572 attenuates Cos2–Smo interaction

We next explored the mechanism by which phosphorylation of Cos2 antagonizes its ability to block Smo. Cos2 blocks Smo phosphorylation through its C-terminal cargo domain, which has been shown to interact with the Smo C-terminal intracellular tail (SmoCT), raising the possibility that binding of Cos2 to Smo could block the accessibility of PKA and CKI to Smo, whereas Fu phosphorylation of Cos2 at Ser572 could attenuate Cos2–Smo interaction, allowing PKA and CKI to phosphorylate Smo. To determine if Ser572 phosphorylation affects direct interaction between Cos2 and SmoCT, we carried out GST pull-down experiments with a purified, bacterially expressed GST-$Smo^{557–686}$ (Ser557 to Asn686) fusion protein and with cell lysates from S2 cells expressing various forms of Cos2. It has been shown that Smo557–686 directly interacts with the Cos2 C-terminal region (Lum et al. 2003). Consistent with this, GST-$Smo^{557–686}$ pulled down the Cos2CT (Fig. 7A, lane 2, top panel) but not the Cos2 microtubule-binding domain (Cos2MD) (Fig. 7A, lane 1, top panel). We also found that both $Cos2^{WT}$ and $Cos2^{S572A}$ associated with GST-$Smo^{557–686}$ strongly (Fig. 7A, lanes 3,4, top panel); however, $Cos2^{S572D}$ was barely precipitated by GST-$Smo^{557–686}$ (Fig. 7A, lane 5, top panel), suggesting that

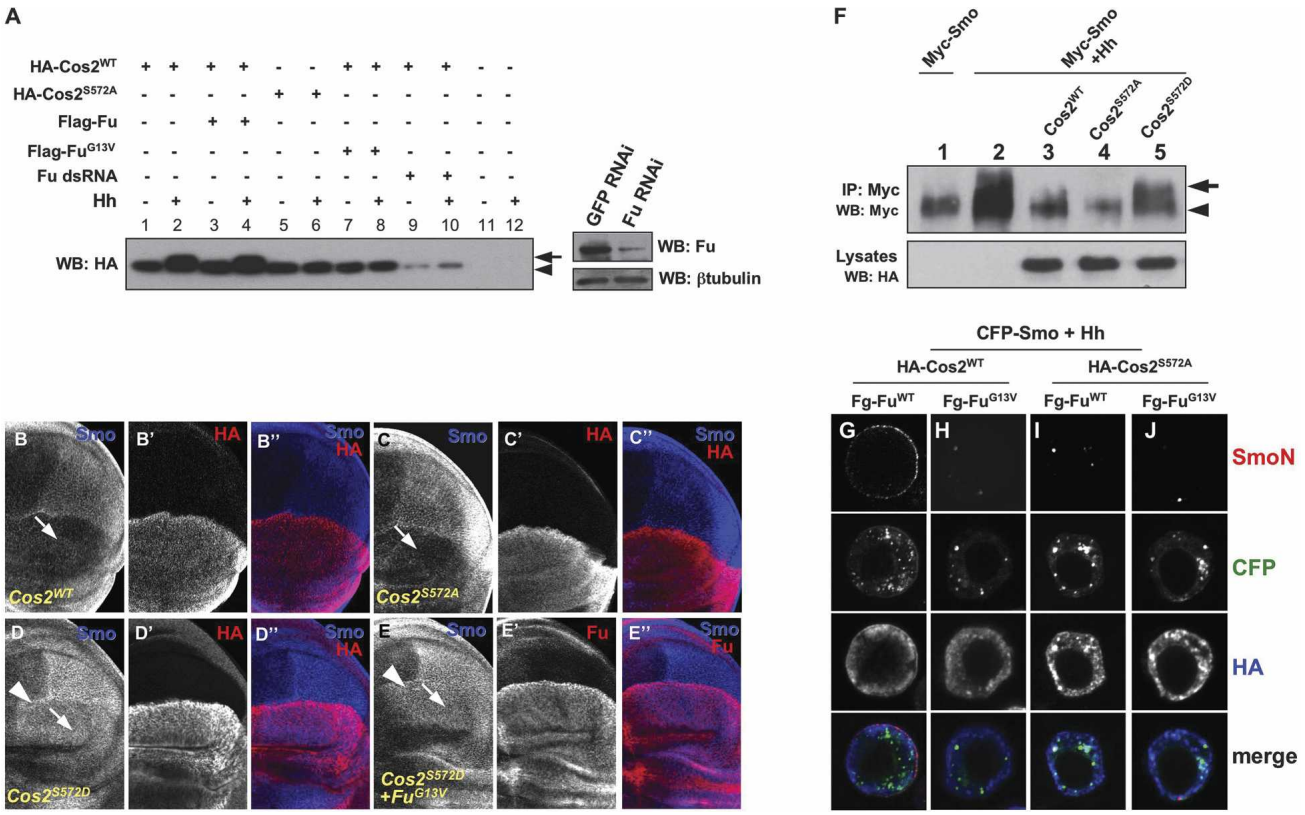

Figure 6. Fu phosphorylation of Cos2 at Ser572 alleviates its inhibition on Smo accumulation. (*A*) S2 cells were transfected with the indicated constructs and treated with Hh-conditioned or control medium. Cell extracts were subjected to direct Western blot with anti-HA antibody to detect the phosphorylation status of Cos2. The arrow indicates hyperphosphorylated forms of Cos2 and the arrowhead indicates hypophosphorylated and unphosphorylated forms. (Lanes *9*,*10*) Of note, Fu RNAi resulted in a reduction in Cos2 level. The efficiency of Fu RNAi is shown in the *right* panel. (*B–D″*) Wing discs expressing HA-Cos2^{WT} (*B–B″*), HA-Cos2^{S572A} (*C–C″*), or HA-Cos2^{S572D} (*D–D″*) by *ap*-Gal4 were immunostained with anti-SmoN (blue) and anti-HA (red) antibodies to show the effects of Cos2 variants on Smo accumulation in dorsal P-cells (arrows). (*E–E″*) A wing disc coexpressing HA-Fu^{G13V} with HA-Cos2^{S572D} was stained with anti-SmoN (blue) and anti-Fu (red) antibodies. (*F*) S2 cells were cotransfected with Myc-tagged Smo and HA-tagged Cos2 mutants and treated with Hh-conditioned or control medium. (*Top* panel) Cell extracts were immunoprecipitated with anti-Myc antibody and Western-blotted with anti-Myc antibody to show the effects of Cos2 on Smo phosphorylation. The arrow indicates hyperphosphorylated forms of Smo and the arrowhead indicates hypophosphorylated and unphosphorylated forms. (*Bottom* panel) Lysates were subjected to direct Western blot with anti-HA antibody to show the expression of Cos2. Double the amount of the Cos2^{S572D} cDNA construct was used in cotransfection to normalize Cos2 protein levels. (*G–J*) S2 cells were cotransfected with different combinations of the indicated constructs and treated with Hh-conditioned medium, followed by the cell-based assay to detect cell-surface-localized Smo. The expression of HA-tagged Cos2 constructs was visualized by anti-HA staining (blue).

Ser572 phosphorylation prevents Cos2 from binding directly to the membrane-proximal region of SmoCT.

Cos2 Ser572 phosphorylation promotes Cos2 degradation

When we examined the effect of Cos2^{S572D} on Smo phosphorylation we noticed that the expression levels of Cos2^{S572D} were consistently low, suggesting that phosphorylation of Cos2 at Ser572 may trigger Cos2 degradation, which may represent an additional mechanism to alleviate Smo from Cos2 inhibition. We first examined the relative stability of Cos2^{WT}, Cos2^{S572A}, and Cos2^{S572D} proteins in S2 cells. S2 cells were transfected with constructs expressing each of these Cos2 variants, and Cos2 protein levels were monitored at different time points after the treatment with the protein synthesis inhibitor, cycloheximide. We found that little Cos2^{S572D} was detectable after 4 h of incubation with cycloheximide (Fig. 7C, lane 9). In contrast, the Ser572Ala mutation made Cos2 protein more stable (Fig. 7C, lanes 4–6) compared with Cos2^{WT} (Fig. 7C, lanes 1–3). This was further demonstrated by a quantification analysis (Fig. 7D). These data support the idea that Ser572 phosphorylation by Fu destabilizes Cos2.

To determine if Fu regulates Cos2 stability in response to Hh, we cotransfected S2 cells with Cos2-, Fu-, and Smo-expressing constructs, followed by treatment with Hh-conditioned or control medium. As shown in Figure 7E, Flag-tagged wild-type Fu (Fg-Fu^{WT}) promoted HA-Cos2^{WT} degradation in response to Hh (lane 1). Hh-in-

duced Cos2 instability depended on Fu kinase activity, as the kinase-dead, dominant-negative Fu^{G13V} stabilized HA-$Cos2^{WT}$ in response to Hh (Fig. 7E, lane 7). Hh-induced Cos2 instability also depended on Ser572 phosphorylation by Fu, as the stability of HA-$Cos2^{S572A}$ remained nearly unchanged regardless of Hh stimulation. On the other hand, HA-$Cos2^{S572D}$ was unstable under these conditions.

To determine if Fu regulates Cos2 stability in vivo, we examined Cos2 distribution in wing discs expressing the dominant-negative Fu^{G13V} or Fu^{WT}. It has been shown that Hh induces Cos2 instability in both embryos and imaginal discs (Ruel et al. 2003) so that the cells in the P-compartment or the A-compartment abutting the A/P boundary exhibit low levels of Cos2. We found that expression of Fu^{G13V} stabilized Cos2 in the P-compartment (Fig. 7F, arrow), but expression of Fu^{WT} did not (Fig. 7G, arrow), suggesting that Hh-induce Cos2 instability is mediated by Fu in vivo. Furthermore, we found that expression of Fu^{WT} promoted Cos2 turnover in A-cells adjacent to the A/P boundary but not in A-cells distant from the A/P boundary (Supplementary Fig. S5B), suggesting that the ability of Fu to promote Cos2 instability depends on Hh.

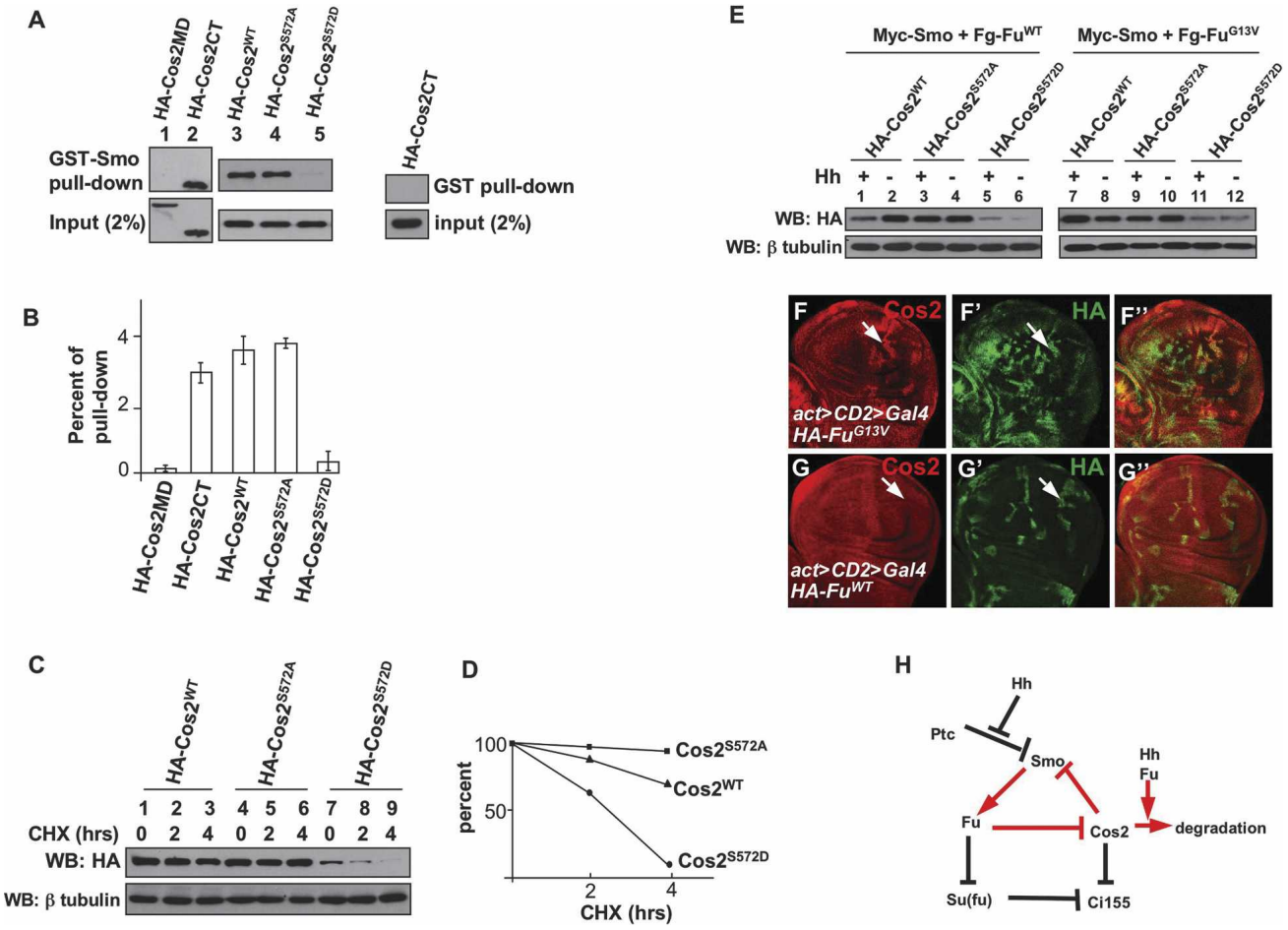

Figure 7. Cos2 phosphorylation at Ser572 attenuates Cos2–Smo interaction and promotes Cos2 degradation. (*A*) Extracts from S2 cells expressing the indicated HA-tagged Cos2 constructs were incubated with GST-$Smo^{557–686}$ fusion protein. (*Top* panel) The bound Cos2 proteins were analyzed by Western blot with anti-HA antibody. (*Bottom* panel) Equal amounts of GST-$Smo^{557–686}$ fusion protein and equal amounts of input Cos2 protein were used. (*Right* panel) The interaction between GST and Cos2CT served as a negative control. (*B*) Quantification of Cos2 variants associated with GST-$Smo^{557–686}$. The pull-down efficiency was determined by the amount of bound Cos2 divided by the amount of total input. Three independent experiments were performed. (*C*, *top* panel) The stability of $Cos2^{WT}$, $Cos2^{S572A}$, and $Cos2^{S572D}$ in transfected S2 cells was analyzed by direct Western blot with anti-HA antibody after incubation with cycloheximide for the indicated times. (*Bottom* panel) The β-tubulin levels served as loading control. (*D*) Quantification of $Cos2^{WT}$, $Cos2^{S572A}$, and $Cos2^{S572D}$ by Western analysis performed in *C*. (*E*) S2 cells were transfected with the indicated constructs and treated with Hh-conditioned or control medium. Cell lysates were subjected to direct Western blot with anti-HA antibody to detect Cos2 protein levels. β-tubulin served as a loading control. (*F–G″*) Wing discs expressing HA-Fu^{G13V} (*F–F″*) or HA-Fu^{WT} (*G–G″*) by *act* > *CD2* > Gal4 were immunostained for HA (green) and Cos2 (red). (*H*) A model for regulating Smo phosphorylation and accumulation by a positive feedback loop. Fu is required for Hh-induced Smo phosphorylation and accumulation through antagonizing the inhibitory role of Cos2. By phosphorylating Cos2 at Ser572, Fu kinase prevents Cos2 from inhibiting Smo, which attenuates Cos2–Smo interaction and promotes Cos2 degradation.

Discussion

The seven-transmembrane protein Smo plays a central role in transducing the Hh signal. In this study, we demonstrate that Fu kinase is essential for Smo phosphorylation and cell-surface accumulation. We further show that the Fu kinase acts through phosphorylation of Cos2 at Ser572, which releases an inhibition of Smo phosphorylation imposed by Cos2. Thus, our study provides the first evidence for a physiologically relevant Fu substrate, and uncovers a feedback mechanism by which Fu promotes Smo hyperphosphorylation and cell-surface accumulation, which is essential for optimal Hh pathway activation (Fig. 7H). Mechanistically, we provide evidence that Cos2 blocks Smo phosphorylation through direct binding to Smo, and that Cos2 Ser572 phosphorylation by Fu attenuates Cos2–Smo interaction and induces Cos2 protein degradation, both of which may contribute to the alleviation of Cos2 inhibition on Smo. Our study thus unravels an unanticipated layer of Smo regulation by the downstream Hh signaling complex.

Opposing roles of Fu and Cos2 in regulating Smo

Fu is characterized as a positive regulator in Hh signal transduction (Ohlmeyer and Kalderon 1998; Wang et al. 2000; Lefers et al. 2001). In the absence of Hh, Fu is required for Ci sequestration in the cytoplasm, whereas in the presence of Hh, it is required for Ci nuclear translocation (Wang and Holmgren 2000; Wang et al. 2000). The finding that Smo directly interacts with the Cos2–Fu protein complex even in the absence of the Hh signal prompted us to further dissect the role of this complex in regulating Hh signal transduction. Unexpectedly, we found that overexpression of a kinase-dead, dominant-negative form of Fu blocked Hh-induced Smo accumulation in both S2 cells and wing discs. Furthermore, we found Hh-induced Smo accumulation was blocked in *fu* mutant clones in wing discs. However, overexpressing Fu alone does not induce Smo accumulation in A-cells away from the A/P boundary (Supplementary Fig. S5A), and does not promote Smo phosphorylation in S2 cells (data not shown). These results suggest that Fu plays a positive role in regulating Smo cell-surface accumulation and this regulation depends on Hh.

The blockade of Smo accumulation in the absence of Fu activity appears to be mediated by Cos2, as removal of Cos2 from Fu^{G13V}-expressing cells by genetic mutation or RNAi restored Hh-induced Smo accumulation (Fig. 3B,E). Furthermore, Hh-induced Smo accumulation is restored in *fu cos2* double-mutant clones (Fig. 3D). These observations suggest that Cos2 normally exerts a negative regulation on Smo, and that this inhibition needs to be alleviated through the Fu kinase activity in order for Hh to induce Smo accumulation and hyperactivation. This mechanism may explain why overexpression of Cos2 in wing discs and S2 cells can block Smo accumulation, as excess amounts of Cos2 can titrate out endogenous Fu, which leads to formation of Smo–Cos2 complexes devoid of Fu and keeps Smo from being activated by Hh.

We found that *fu* clones in P-cells do not show attenuated Smo levels (Fig. 3C–C′′′), which could be due to the highest level of Hh and/or lack of Ptc in these cells so that Smo exists in a hyperphosphorylated and active form and may no longer be subject to the feedback regulation in *fu* mutant clones.

Regulation of Smo phosphorylation by Fu and Cos2

Although Fu^{G13V} and Cos2 can block Hh-induced cell-surface accumulation of wild-type Smo, we found that the phosphorylation-mimicking Smo variant Smo^{SD123}, which exhibits constitutive cell-surface accumulation and signaling activity (Jia et al. 2004), escaped the inhibition by Fu^{G13V} and Cos2 (Figs. 2I,J, 3G), suggesting that the regulation of Smo by Fu and Cos2 is upstream of Smo phosphorylation. Consistent with this idea, we found that overexpressing Fu^{G13V} or Cos2 blocked Hh-induced Smo phosphorylation in S2 cells (Fig. 5A).

We further demonstrated that Cos2 inhibits Hh-induced Smo phosphorylation through its C-terminal Smo-binding domain. We showed that the Cos2 cargo domain from amino acids 990–1201 is both necessary and sufficient for blocking Hh-induced Smo phosphorylation in S2 cells (Fig. 5A). In addition, the Cos2 cargo domain is also necessary and sufficient for blocking Smo accumulation in both wing discs and S2 cells (Fig. 4F; Supplementay Fig. S1). The Cos2 cargo domain has been shown to interact with PKA and CKI (Zhang et al. 2005), raising the possibility that it may inhibit Smo phosphorylation by titrating out these kinases. However, the observation that coexpression of PKA and CKI with Cos2 failed to restore Smo accumulation does not support this model.

It has also been shown that the Cos2 cargo domain mediates binding between Cos2 and Smo (Jia et al. 2003; Lum et al. 2003; Ruel et al. 2003). GST pull-down assays suggest that the Cos2 cargo domain binds the Smo C-terminal region between amino acids 661 and 686 (Lum et al. 2003), which includes the first PKA and CKI phosphorylation cluster. It is possible that binding of Cos2 to this region blocks the access of PKA and/or CKI to their target sites in the Smo C-tail, leading to inhibition of Smo phosphorylation.

Although our data suggest that Cos2 plays an inhibitory role in regulating Smo phosphorylation, removal of Cos2 in the absence of Hh is not sufficient to promote Smo phosphorylation, as A-compartment *cos2* mutant cells situated at a distance from the A/P boundary did not accumulate high levels of Smo (Supplementary Fig. S3A), suggesting that additional mechanism(s) must exist to block Smo phosphorylation in the absence of Hh. An obvious candidate is Ptc, since *ptc* mutant clones situated in the A-compartment of wing discs accumulate high levels of Smo, and RNAi knockdown of *ptc* results in Smo phosphorylation in S2 cells (Zhu et al. 2003; Nakano et al. 2004). Furthermore, the inhibitory effect of Ptc on Smo is further strengthened in *cos2* mutant cells as *ptc* expression is up-regulated in these cells (Zhang et al. 2005).

Fu regulates Smo by phosphorylating Cos2

It has been shown previously that Fu phosphorylates Cos2 at Ser572, which appears to be a major site for Cos2 phosphorylation in response to Hh (Nybakken et al. 2002). We found that the phosphorylation-mimicking Cos2 variant ($Cos2^{S572D}$) no longer blocked Smo phosphorylation and cell-surface accumulation in response to Hh, whereas the phosphorylation-deficient Cos2 variant ($Cos2^{S572A}$) exhibited strong inhibitory activity on Smo phosphorylation (Fig. 6F, cf. lanes 3–5) and cell-surface accumulation (Fig. 6I,J). In S2 cells, the blockade of Smo accumulation by wild-type Cos2 was alleviated by coexpression of Fu; in contrast, the activity of $Cos2^{S572A}$ in blocking Smo was no longer inhibited by Fu coexpression (Fig. 6I). Taken together, these observations suggest that Ser572 phosphorylation is a major regulatory event by which Fu antagonizes the inhibitory activity of Cos2 toward Smo in response to Hh. However, our data do not rule out the possibility that Fu may also exert a direct positive role on Smo; e.g., by phosphorylating Smo.

How does Ser572 phosphorylation of Cos2 alleviate its inhibition on Smo? We found that Ser572 phosphorylation appeared to decrease Cos2–Smo interaction, as $Cos2^{S572D}$ bound poorly to GST-Smo compared with the binding of $Cos2^{WT}$ or $Cos2^{S572A}$ (Fig. 7A). We also found that Ser572 phosphorylation promotes Cos2 instability, although the underlying mechanism is not clear. This conclusion is supported by several lines of evidence. First, $Cos2^{S572D}$ is unstable and has a much shorter half-life than $Cos2^{WT}$ and $Cos2^{S572A}$. Second, Fu^{WT} but not Fu^{G13V} can down-regulate Cos2 in response to Hh, whereas $Cos2^{S572A}$ is resistant to such down-regulation. Third, Hh-induced down-regulation of Cos2 is abolished in wing disc cells expressing Fu^{G13V}, suggesting that Fu kinase activity is required for promoting Cos2 instability in vivo. If binding of Cos2 to Smo contributed to Smo inhibition, as our data suggested, then decreasing Cos2–Smo-binding affinity and promoting Cos2 degradation should spare Smo from being inhibited by Cos2.

It should be noted that Smo can pull down Cos2 and Fu even in the presence of Hh stimulation (Jia et al. 2003; Lum et al. 2003; Ruel et al. 2003), implying that the Cos2–Fu complex can form a stable complex with activated Smo, whereas our results imply that Cos2 dissociates from Smo in response to Hh. How can one reconcile these seemingly contradictory observations? We provide the following explanations. Although Cos2 associates with activated Smo in the presence of Hh, it might bind Smo in a different way from that in the absence of Hh signaling. For example, Cos2 may bind two distinct domains of Smo: one occupied in the absence of Hh and the other in the presence of Hh, with only one of the interactions being disrupted by Fu phosphorylation. Alternatively, Cos2 may bind directly with inactivated Smo, but associate with activated Smo indirectly through other protein(s) such as Fu, as it has been shown recently that Fu can bind directly to the C-terminal region of Smo in a yeast two-hybrid assay (Malpel et al. 2007).

Our data indicate that Fu promotes Cos2 instability in response to Hh by phosphorylating Cos2 Ser572 (Fig. 7E), whereas activated forms of Smo appear to form a stable complex with Cos2–Fu. It is possible that Cos2 degradation might only occur during the process of Smo activation. Once Smo is hyperphosphorylated and fully activated, it might reassociate with Cos2–Fu to form a relatively stable complex. In other words, there could be two distinct pools of Cos2–Fu complexes, one associated with inactive forms of Smo and the other with activated forms of Smo, as implicated by a recent study (Ogden et al. 2006). The pool of Cos2 associated with inactive forms of Smo might dissociate from Smo or get degraded in response to Hh, allowing Smo to be hyperphosphorylated and fully activated. Cos2 associated with the activated forms of Smo might undergo other modification(s), such as additional phosphorylation, that could stabilize it. Alternatively, other factors present in the active or inactive Smo–Cos2–Fu complexes might influence Cos2 stability.

The complex relationship among Smo, Cos2, and Fu

The prevalent view for the role of Fu in the Hh pathway is that it acts downstream from Smo to transduce the Hh signal (Ingham and McMahon 2001; Lum and Beachy 2004; Jia and Jiang 2006). Here we demonstrate that Fu is required to promote Smo phosphorylation and thus activation, therefore placing Fu upstream of Smo. However, activation of Smo is unlikely to account for all the Fu activity in the Hh pathway, as we found that Smo^{SD123}, which is no longer regulated by Fu, still depends on Fu to activate Hh target genes. For example, coexpression of Fu^{G13V} with Smo^{SD123} attenuated Smo^{SD123}-induced *ptc-lacZ* expression and abolished Smo^{SD123}-induced En expression (Supplementary Fig. S4). Hence, we propose that Fu plays a dual role in both activating Smo and transducing the Hh signal downstream from Smo (Fig. 7H). One possible Fu substrate downstream from Smo is Su(fu). Genetic studies suggest that Fu activates Ci by antagonizing Su(fu) (Ohlmeyer and Kalderon 1998). In addition, Hh-induced Su(fu) phosphorylation depends on Fu (Lum et al. 2003).

Cos2 phosphorylation by Fu at Ser572 may also inhibit its activity toward promoting Ci processing, as $Cos2^{Ser572D}$ failed to restore Ci processing in *cos2* mutant wing discs (Supplementary Fig. S3D′). In addition, $Cos2^{Ser572D}$ has a dominant-negative effect over endogenous Cos2 and blocks Ci processing, leading to partial activation of the Hh pathway (Supplementary Fig. S2D; data not shown). Thus, Fu phosphorylation of Cos2 at Ser572 may prevent Cos2 from inhibiting both Smo and Ci. Further studies are needed to investigate the mechanism by which Ser572 phosphorylation of Cos2 inhibits its activity in promoting Ci processing.

The Hh signal transduction pathway between Smo and Ci/Gli appears to diverge between insects and mammals (Huangfu and Anderson 2006). Most notably, targeted disruption of the mammalian homolog of Fu (mFu) failed to reveal any defects in Hh signaling, although one cannot rule out the possibility that a distant relative of mFu

could compensate for the loss of mFu (Chen et al. 2005; Merchant et al. 2005). Similarly, a study in cultured cells using RNAi failed to reveal a role of mammalian Cos2 homologs (Kif7 and Kif27) in Shh singaling (Varjosalo et al. 2006). Thus, the feedback mechanism involving Fu and Cos2 in regulating Smo may not apply to the mammalian system. It has been shown that mammalian Smo (mSmo) translocates to the primary cilium in response to Hh, although the underlying regulatory mechanism remains poorly understood. It is not impossible that mSmo might be regulated by an analogous feedback mechanism.

Materials and methods

Mutants and transgenes

fu^A is a strong *fu* mutant allele with a deletion in the extracatalytic domain (Alves et al. 1998), and *fu^{mH63}* is a strong hypomorphic allele (Preat 1992). *$cos2^2$* is a null allele (Sisson et al. 1997). *MS1096*, *act > CD2 > Gal4*, *armadillo-Gal4*, *ap*-Gal4, *UAS-mC**, *UAS-Fg-CKIα*, *UAS-hh*, and *ptc-lacZ* have been described (Li et al. 1995; Jia et al. 2004, 2005; FlyBase at http://flybase.bio.indiana.edu). A Fu mutation with substitution of Gly13 to Val and Cos2 mutations with substitutions at Ser572 were generated by site-directed mutagenesis. To construct *UAS-HA-Fu^{WT}* and *UAS-HA-Fu^{G13V}*, two copies of an HA tag were inserted at the N termini of Fu, and the fusion gene was subcloned into the vector pUAST between the EcoRI and NotI sites. *UAS-Flag-Fu^{WT}* (*Fg-Fu^{WT}*) and *UAS-Flag-Fu^{G13V}* (*Fg-Fu^{G13V}*) were constructed with three copies of a Flag tag inserted at the N termini of Fu and subcloned into pUAST between the EcoRI and NotI sites. The Myc-Fu construct contains six copies of a Myc tag inserted at the N terminus of Fu and was subcloned into pUAST between the EcoRI and NotI sites. Myc-Smo, HA-$Cos2^{WT}$, HA-Cos2ΔN1, HA-Cos2ΔN2, HA-Cos2MD, HA-Cos2ΔC1, and HA-Cos2CT have been described (Wang et al. 2000; Jia et al. 2003). HA-$Cos2^{S572A}$ and HA-$Cos2^{S572D}$ were generated using the same approach. HA-Cos2ΔC1^{S572A} and HA-Cos2ΔC1^{S572D} were constructed by swapping the domains from HA-$Cos2^{S572A}$ and HA-$Cos2^{S572D}$ using the endogenous HindIII site at amino acid 791. HA-Cos2ΔC2 was derived from HA-$Cos2^{WT}$ by introducing a stop codon after amino acid 642. pUAST-Myc has six copies of a Myc tag inserted into the pUAST vector between EcoRI and BglII. Fly transformants were generated by standard P-element-mediated transformation. Multiple independent transgenic lines were generated and examined for each construct.

Cell culture, transfection, immunoprecipitation, and Western blot analysis

S2 cells were cultured in Schneider's *Drosophila* Medium (Invitrogen) with 10% fetal bovine serum, 100 U/mL penicillin, and 100 µg/mL streptomycin. Transfection, immunoprecipitation, and immunoblot analysis were performed with standard protocols as described previously (Jia et al. 2004). The cell-based assay to detect Smo cell-surface accumulation was carried out by immunostaining with anti-SmoN antibody before cell permeabilization (Jia et al. 2004). Fu and Cos2 dsRNA were synthesized against the regions described previously (Lum et al. 2003; Ruel et al. 2003) and used for both treatment and transfection to get better interference with the endogenous protein expression. Control GFP dsRNA was synthesized against EGFP amino acids 2–201. Cycloheximide (Sigma) treatment was performed at a final concentration of 100 µM for the indicated time periods before harvesting S2 cells. Antibodies used in this study were mouse anti-Myc, 9E10 (Santa Cruz Biotechnology), anti-HA, F7 (Santa Cruz Biotechnology), anti-Flag, M2 (Sigma), anti-Cos2 (gift from D. Robbins), anti-SmoN (Developmental Studies Hybridoma Bank [DSHB]), anti-βtubulin (DSHB); rabbit anti-Fu (gift from D. Robbins), anti-PKA (Santa Cruz Biotechnology), and anti-HA, Y-11 (Santa Cruz Biotechnology).

GST fusion protein pull-down assay

GST fusion proteins were produced from *Escherichia coli* lysates. Equal amount of GST-Smo fusion protein or GST protein were incubated with glutathione-Sepharose 4B beads and washed in phosphate-buffered saline. GST-fusion protein-loaded beads were incubated with S2 cell lysates with equal amounts of HA-tagged Cos2 proteins for 2 h at 4°C, followed by four 10-min washes with lysis buffer and then by Western blot analysis to detect the bound Cos2 proteins. To normalize the protein levels, GST-Smo or GST was stained with Commassie blue and their intensity was calculated by Metamorph software. To normalize the amount of input $Cos2^{WT}$, $Cos2^{S572A}$, and $Cos2^{S572D}$ protein, cell lysates from S2 cells expressing Cos2 variants were subjected to direct Western blot with anti-HA antibody and were analyzed by Metamorph software to make the input of Cos2 proteins equal. HA-$Cos2^{WT}$ and HA-$Cos2^{S572A}$ lysates were diluted with nontransfection S2 cells lysates.

Immunostaining of imaginal discs

Standard protocols for immunofluorescence staining of imaginal discs were used (Jiang and Struhl 1995) with the antibodies mouse anti-Myc, 9E10 (Santa Cruz Biotechnology), anti-HA, F7 (Santa Cruz Biotechnology), anti-Flag, M2 (Sigma), anti-Cos2, 5D6 (gift from D. Robbins), anti-En (DSHB), anti-SmoN (DSHB), anti-Ptc (DSHB); rabbit anti-Fu (gift from D. Robbins), anti-PKA (Santa Cruz Biotechnology), anti-Flag (ABR), anti-HA, Y-11 (Santa Cruz Biotechnology), anti-βGal (Cappel), anti-GFP (Clontech), and rat anti-Ci, 2A (gift from R. Holmgren).

Acknowledgments

We thank Drs. Robert Holmgren, David J. Robbins, Daniel Kalderon, Anne Plessis, and Jingwu Xie for providing valuable reagents. We are grateful to Drs. Mark Evers, David Konkel, and Cornelis Elferink for critically reading the manuscript. We also thank Drs. Chunming Liu, Peter Zhou, and Tianyan Gao for helpful discussions. This work was supported by grants from John Sealy Memorial Fund and American Cancer Society Institutional Research Award to J. Jia. J. Jiang is supported by grants from the National Institutes of Health, the Leukemia and Lymphoma Society Scholar Program, and the Robert A. Welch Foundation.

References

Alves, G., Limbourg-Bouchon, B., Tricoire, H., Brissard-Zahraoui, J., Lamour-Isnard, C., and Busson, D. 1998. Modulation of Hedgehog target gene expression by the Fused serine–threonine kinase in wing imaginal discs. *Mech. Dev.* **78:** 17–31.

Apionishev, S., Katanayeva, N.M., Marks, S.A., Kalderon, D., and Tomlinson, A. 2005. *Drosophila* Smoothened phos-

phorylation sites essential for Hedgehog signal transduction. *Nat. Cell Biol.* **7:** 86–92.

Aza-Blanc, P., Ramirez-Weber, F.A., Laget, M.P., Schwartz, C., and Kornberg, T.B. 1997. Proteolysis that is inhibited by hedgehog targets Cubitus interruptus protein to the nucleus and converts it to a repressor. *Cell* **89:** 1043–1053.

Chen, C.H., von Kessler, D.P., Park, W., Wang, B., Ma, Y., and Beachy, P.A. 1999. Nuclear trafficking of Cubitus interruptus in the transcriptional regulation of Hedgehog target gene expression. *Cell* **98:** 305–316.

Chen, M.H., Gao, N., Kawakami, T., and Chuang, P.T. 2005. Mice deficient in the fused homolog do not exhibit phenotypes indicative of perturbed hedgehog signaling during embryonic development. *Mol. Cell. Biol.* **25:** 7042–7053.

Denef, N., Neubuser, D., Perez, L., and Cohen, S.M. 2000. Hedgehog induces opposite changes in turnover and subcellular localization of patched and smoothened. *Cell* **102:** 521–531.

Ho, K.S., Suyama, K., Fish, M., and Scott, M.P. 2005. Differential regulation of Hedgehog target gene transcription by Costal2 and Suppressor of Fused. *Development* **132:** 1401–1412.

Huangfu, D. and Anderson, K.V. 2006. Signaling from Smo to Ci/Gli: Conservation and divergence of Hedgehog pathways from *Drosophila* to vertebrates. *Development* **133:** 3–14.

Ingham, P.W. and McMahon, A.P. 2001. Hedgehog signaling in animal development: Paradigms and principles. *Genes & Dev.* **15:** 3059–3087.

Jia, J. and Jiang, J. 2006. Decoding the Hedgehog signal in animal development. *Cell. Mol. Life Sci.* **63:** 1249–1265.

Jia, J., Tong, C., and Jiang, J. 2003. Smoothened transduces Hedgehog signal by physically interacting with Costal2/Fused complex through its C-terminal tail. *Genes & Dev.* **17:** 2709–2720.

Jia, J., Tong, C., Wang, B., Luo, L., and Jiang, J. 2004. Hedgehog signalling activity of Smoothened requires phosphorylation by protein kinase A and casein kinase I. *Nature* **432:** 1045–1050.

Jia, J., Zhang, L., Zhang, Q., Tong, C., Wang, B., Hou, F., Amanai, K., and Jiang, J. 2005. Phosphorylation by Double-Time/CKIε and CKIα targets Cubitus interruptus for Slimb/β-TRCP-mediated proteolytic processing. *Dev. Cell* **9:** 819–830.

Jiang, J. and Struhl, G. 1995. Protein kinase A and hedgehog signaling in *Drosophila* limb development. *Cell* **80:** 563–572.

Lefers, M.A., Wang, Q.T., and Holmgren, R.A. 2001. Genetic dissection of the *Drosophila* Cubitus interruptus signaling complex. *Dev. Biol.* **236:** 411–420.

Li, W., Ohlmeyer, J.T., Lane, M.E., and Kalderon, D. 1995. Function of protein kinase A in hedgehog signal transduction and *Drosophila* imaginal disc development. *Cell* **80:** 553–562.

Lum, L. and Beachy, P.A. 2004. The Hedgehog response network: Sensors, switches, and routers. *Science* **304:** 1755–1759.

Lum, L., Zhang, C., Oh, S., Mann, R.K., von Kessler, D.P., Taipale, J., Weis-Garcia, F., Gong, R., Wang, B., and Beachy, P.A. 2003. Hedgehog signal transduction via Smoothened association with a cytoplasmic complex scaffolded by the atypical kinesin, Costal-2. *Mol. Cell* **12:** 1261–1274.

Malpel, S., Claret, S., Sanial, M., Brigui, A., Piolot, T., Daviet, L., Martin-Lanneree, S., and Plessis, A. 2007. The last 59 amino acids of Smoothened cytoplasmic tail directly bind the protein kinase Fused and negatively regulate the Hedgehog pathway. *Dev. Biol.* **303:** 121–133.

Merchant, M., Evangelista, M., Luoh, S.M., Frantz, G.D., Chalasani, S., Carano, R.A., van Hoy, M., Ramirez, J., Ogasawara, A.K., McFarland, L.M., et al. 2005. Loss of the serine/threonine kinase fused results in postnatal growth defects and lethality due to progressive hydrocephalus. *Mol. Cell. Biol.* **25:** 7054–7068.

Methot, N. and Basler, K. 1999. Hedgehog controls limb development by regulating the activities of distinct transcriptional activator and repressor forms of Cubitus interruptus. *Cell* **96:** 819–831.

Methot, N. and Basler, K. 2000. Suppressor of fused opposes hedgehog signal transduction by impeding nuclear accumulation of the activator form of Cubitus interruptus. *Development* **127:** 4001–4010.

Monnier, V., Ho, K.S., Sanial, M., Scott, M.P., and Plessis, A. 2002. Hedgehog signal transduction proteins: Contacts of the Fused kinase and Ci transcription factor with the kinesin-related protein Costal2. *BMC Dev. Biol.* **2:** 4. doi: 10.1186/1471-213X-2-4.

Nakano, Y., Nystedt, S., Shivdasani, A.A., Strutt, H., Thomas, C., and Ingham, P.W. 2004. Functional domains and subcellular distribution of the Hedgehog transducing protein Smoothened in *Drosophila*. *Mech. Dev.* **121:** 507–518.

Nybakken, K.E., Turck, C.W., Robbins, D.J., and Bishop, J.M. 2002. Hedgehog-stimulated phosphorylation of the kinesin-related protein Costal2 is mediated by the serine/threonine kinase fused. *J. Biol. Chem.* **277:** 24638–24647.

Ogden, S.K., Ascano Jr., M., Stegman, M.A., Suber, L.M., Hooper, J.E., and Robbins, D.J. 2003. Identification of a functional interaction between the transmembrane protein Smoothened and the kinesin-related protein Costal2. *Curr. Biol.* **13:** 1998–2003.

Ogden, S.K., Casso, D.J., Ascano Jr., M., Yore, M.M., Kornberg, T.B., and Robbins, D.J. 2006. Smoothened regulates activator and repressor functions of Hedgehog signaling via two distinct mechanisms. *J. Biol. Chem.* **281:** 7237–7243.

Ohlmeyer, J.T. and Kalderon, D. 1998. Hedgehog stimulates maturation of Cubitus interruptus into a labile transcriptional activator. *Nature* **396:** 749–753.

Pasca di Magliano, M. and Hebrok, M. 2003. Hedgehog signalling in cancer formation and maintenance. *Nat. Rev. Cancer* **3:** 903–911.

Preat, T. 1992. Characterization of Suppressor of fused, a complete suppressor of the fused segment polarity gene of *Drosophila melanogaster*. *Genetics* **132:** 725–736.

Preat, T., Therond, P., Limbourg-Bouchon, B., Pham, A., Tricoire, H., Busson, D., and Lamour-Isnard, C. 1993. Segmental polarity in *Drosophila melanogaster*: Genetic dissection of fused in a Suppressor of fused background reveals interaction with costal-2. *Genetics* **135:** 1047–1062.

Price, M.A. 2006. CKI, there's more than one: Casein kinase I family members in Wnt and Hedgehog signaling. *Genes & Dev.* **20:** 399–410.

Robbins, D.J., Nybakken, K.E., Kobayashi, R., Sisson, J.C., Bishop, J.M., and Therond, P.P. 1997. Hedgehog elicits signal transduction by means of a large complex containing the kinesin-related protein costal2. *Cell* **90:** 225–234.

Ruel, L., Rodriguez, R., Gallet, A., Lavenant-Staccini, L., and Therond, P.P. 2003. Stability and association of Smoothened, Costal2 and Fused with Cubitus interruptus are regulated by Hedgehog. *Nat. Cell Biol.* **5:** 907–913.

Sisson, J.C., Ho, K.S., Suyama, K., and Scott, M.P. 1997. Costal2, a novel kinesin-related protein in the Hedgehog signaling pathway. *Cell* **90:** 235–245.

Stegman, M.A., Vallance, J.E., Elangovan, G., Sosinski, J., Cheng, Y., and Robbins, D.J. 2000. Identification of a tetrameric hedgehog signaling complex. *J. Biol. Chem.* **275:** 21809–21812.

Strigini, M. and Cohen, S.M. 1997. A Hedgehog activity gradi-

ent contributes to AP axial patterning of the *Drosophila* wing. *Development* **124:** 4697–4705.
Taipale, J. and Beachy, P.A. 2001. The Hedgehog and Wnt signalling pathways in cancer. *Nature* **411:** 349–354.
Therond, P., Alves, G., Limbourg-Bouchon, B., Tricoire, H., Guillemet, E., Brissard-Zahraoui, J., Lamour-Isnard, C., and Busson, D. 1996. Functional domains of fused, a serine–threonine kinase required for signaling in *Drosophila*. *Genetics* **142:** 1181–1198.
Tian, L., Holmgren, R.A., and Matouschek, A. 2005. A conserved processing mechanism regulates the activity of transcription factors Cubitus interruptus and NF-κB. *Nat. Struct. Mol. Biol.* **12:** 1045–1053.
Varjosalo, M., Li, S.P., and Taipale, J. 2006. Divergence of hedgehog signal transduction mechanism between *Drosophila* and mammals. *Dev. Cell* **10:** 177–186.
Wang, Q.T. and Holmgren, R.A. 1999. The subcellular localization and activity of *Drosophila* cubitus interruptus are regulated at multiple levels. *Development* **126:** 5097–5106.
Wang, Q.T. and Holmgren, R.A. 2000. Nuclear import of cubitus interruptus is regulated by hedgehog via a mechanism distinct from Ci stabilization and Ci activation. *Development* **127:** 3131–3139.
Wang, G. and Jiang, J. 2004. Multiple Cos2/Ci interactions regulate Ci subcellular localization through microtubule dependent and independent mechanisms. *Dev. Biol.* **268:** 493–505.
Wang, B. and Li, Y. 2006. Evidence for the direct involvement of βTrCP in Gli3 protein processing. *Proc. Natl. Acad. Sci.* **103:** 33–38.
Wang, G., Amanai, K., Wang, B., and Jiang, J. 2000. Interactions with Costal2 and suppressor of fused regulate nuclear translocation and activity of cubitus interruptus. *Genes & Dev.* **14:** 2893–2905.
Zhang, C., Williams, E.H., Guo, Y., Lum, L., and Beachy, P.A. 2004. Extensive phosphorylation of Smoothened in Hedgehog pathway activation. *Proc. Natl. Acad. Sci.* **101:** 17900–17907.
Zhang, W., Zhao, Y., Tong, C., Wang, G., Wang, B., Jia, J., and Jiang, J. 2005. Hedgehog-regulated Costal2–kinase complexes control phosphorylation and proteolytic processing of Cubitus interruptus. *Dev. Cell* **8:** 267–278.
Zhu, A.J., Zheng, L., Suyama, K., and Scott, M.P. 2003. Altered localization of *Drosophila* Smoothened protein activates Hedgehog signal transduction. *Genes & Dev.* **17:** 1240–1252.